Upright stance is controlled close to critical stability across different postures

Yang Geng[1], Sjoerd M. Bruijn[1], Jaap H. van Dieen[1]*

[1]Department of Human Movement Sciences, Faculty of Behavioral and Movement Sciences, Amsterdam Movement Sciences, Vrije Universiteit Amsterdam, Amsterdam, The Netherlands

Corresponding author: prof. dr. Jaap H. van Dieen; j.van.dieen@vu.nl

Abstract

Feedback stabilization of upright standing postures should be reflected by a time-lagged relationship between the ground reaction force (GRF) and the center of mass (COM) state. In this study, we propose a model relating corrective ground reaction forces (F_{corr}) to preceding COM position (PCOM) and velocity (VCOM). We first checked the model's validity by simulating an inverted pendulum model with known intrinsic and feedback parameters, to see if we could identify the feedback parameters. Next, we tested this model in 14 young adult volunteers standing in different postures.

Our model effectively reconstructed F_{corr} in both simulations (R^2: 0.50~0.99) and human experimental data (R^2: 0.76~0.99). Strikingly, estimated position and velocity gains were similar across postures even between bipedal and unipedal standing, with the position gain slightly above critical stiffness. The estimated delay in normal standing (246±21ms) was significantly larger than that in unipedal standing and step posture (204±24ms and 193±29ms, respectively).

In conclusion, our results support that an estimate of the COM state is used to generate corrective ground reaction forces to stabilize upright posture, and our feedback model can be used to characterize this control mechanism. The proposed model requires only easily measurable inputs which may yield value in assessment of balance disorders. Notably, our results showed that stability of upright stance is achieved by maintaining feedback gains at levels just above critical stability.

Introduction

Even when we are "standing still", our bodies are never completely static and display subtle sway. This continuous body sway is primarily attributable to two factors: 1) the mechanically unstable properties of the segmented human body, where the center of mass (COM) is located high above the relatively small base of support (BOS), and 2) the continuously occurring internal (e.g., respiratory activity and neuromuscular noise) and external (e.g., airflow, moving surfaces, being pushed or jostled) perturbations. In the absence of appropriate corrections, such perturbations may result in a loss of stability and a subsequent fall.

Stabilization of an inverted pendulum, that is, controlling its COM relative to the base of support, can be achieved by feedback control based on the COM state (i.e. its position and velocity) (Pai & Patton, 1997). Indeed, a time-lagged relationship between EMG or joint moments (Afschrift, De Groote, & Jonkers, 2021; Safavynia & Ting, 2013; Welch & Ting, 2008) and COM state has been observed in perturbed human standing. Specifically, a linear feedback model with delayed deviation of COM state as independent variable explained more than 23% of variance of the reactive muscle activity (Safavynia & Ting, 2013; Welch & Ting, 2008) and 94% of variance of the reactive ankle moments (Afschrift et al., 2021) after perturbations of standing.

However, it is obvious that humans not only use active feedback control to stabilize standing posture, as passive mechanisms (i.e., intrinsic stiffness, damping, inertia) also play a role (Amiri, Mohebbi, & Kearney, 2019; Peterka, 2002). Muscles provide short-range intrinsic stiffness, which will generate instantaneous torque to resists movement prior to any involvement of the nervous system (De Groote, Allen, & Ting, 2017). In addition, muscle's length-velocity-force relationship provides effects which can be modeled as stiffness and damping (de Vlugt et al., 2011; Latash & Zatsiorsky, 1993; Rack & Westbury, 1974). The impedance determined by the intrinsic properties of muscles acts in parallel with active feedback control, which may make estimating the active component hard, especially in natural standing without any perturbations. Moreover, human stability control may be intermittent, with a "switch-like" controller, where feedback is only present when the body sways beyond a certain area (dead zone) (De Groote et al., 2017; Kelton & Wright, 1949; Loram, Gollee, van de Kamp, & Gawthrop, 2022; Milton, Townsend, King, & Ohira, 2009). Such intermittent characteristics potentially cause additional challenges when trying to estimate feedback control parameters from unperturbed human standing.

Since any control or stabilization of the COM state should ultimately be reflected in horizontal ground reaction forces, we hypothesize that stability control in

standing can be represented by a linear relationship between the corrective ground reaction force and the preceding COM state. Such a relationship has recently been modeled in a study on unperturbed walking (van Dieen, Bruijn, & Afschrift, 2024). In this study, the COM state during unperturbed walking was shown to predict the ground reaction force after some delay. This suggests that (at least during walking) not only during or shortly after perturbations, delayed feedback control based on COM information is present. If a similar model can be used to characterize control of standing, it can be estimated from easily obtainable data measured during unperturbed standing: COM position and velocity on one hand, and horizontal ground reaction forces or COM acceleration on the other hand.

We here propose to use a simplified feedback model to estimate the feedback parameters, in spite of the intermittent characteristic of human stability control, and the presence of intrinsic stiffness and damping. First, we asked whether meaningful information on feedback gains and delays can be derived from our model fitted to data generated by simulations of a feedback controlled inverted pendulum model, in the presence of independently changed intrinsic and feedback parameters, sensorimotor noise and intermittence. If our results show that corrective ground reaction forces can be well reconstructed from the preceding COM state in these simulations, this indicates that this method may be applicable to investigate feedback control in humans. The simulation results showed that the estimated feedback parameters were highly correlated with the actual feedback parameters. Next, we applied the model to experimental data from human volunteers to assess the feedback model in humans.

In everyday life, we adopt a range of standing postures that suit specific environmental contexts. These postures differ in the size of the area of the base of support (e.g. standing on the full foot versus on tip-toe), and in the structural stiffness provided by the geometry of the legs, as when standing with the feet parallel versus in a step posture. We asked whether changes in standing postures, which are expected to affect stability demands as well as intrinsic stiffness and damping, would cause changes in estimated feedback delays and gains. We fitted the control model to data from different postures (i.e., normal standing, unipedal standing, step posture) to test our methods and investigate how feedback parameters vary over different postures.

Methods

Model simulation

In this study, we limit our analysis to body sway in the anterior-posterior (AP) direction, modeling the human body as an inverted pendulum (IP) oscillating around the ankle, controlled by intrinsic and feedback properties, as illustrated in Figure 1 and equation (1).

The feedback mechanism generates a feedback moment (M_{fd}), which is angle (θ) and angular velocity ($\dot{\theta}$) dependent, with a delay (τ). Both for the angle and angular velocity, there can be a dead zone ($\theta_d,\ \dot{\theta}_d$) acting as a switch of feedback control. When the body sways within these thresholds, no feedback will be provided, while when either of these thresholds is exceeded, position- and/or velocity-dependent feedback will be provided. In effect, the system becomes intermittently controlled.

For the intrinsic and feedback control parameters, previous studies have reported a wide range of values. For example, intrinsic stiffness ranges from relatively low (0.7~2.3 Nm/deg) as reported by Peterka (2002), to substantially higher (10~12 Nm/deg) as reported by Loram and Lakie (2002). Similarly, reported intrinsic damping varies widely, from lower than 0.1 Nms/deg (Loram & Lakie, 2002; Ribeiro, Knop, & Rastgaar, 2020), to much higher values of 1.8~2.2 Nms/deg (Sakanaka, Gill, Lakie, & Reynolds, 2018). Feedback position gain has been reported within a range of 10~20 Nm/deg, while feedback velocity gain has been found to vary from 3.5 to 7 Nms/deg in free standing (Peterka, 2002). In our study, the initial parameters were set to the mean values reported by Peterka (2002), as this allows us to use both feedback and intrinsic parameter estimates from one single study.

For the other model parameters, the default feedback delay was set at 150ms, as a 150~200ms delay has been reported in previous studies (Casadio, Morasso, & Sanguineti, 2005; Peterka, 2002). The default dead zone for position was set as 0.23 deg, which is the same values used by Asai et al. (2009), and for velocity it was accordingly set at 0.092π *deg/s* based on the physical relationship between position and velocity assuming a dominant sway frequency of 0.2 Hz (Peterka, 2002). For the sensorimotor noise, we injected low-pass filtered (5 Hz) random noise with an amplitude of 10 Nm, making the mean sway RMS a bit higher than 0.28 deg (Winter, Patla, Rietdyk, & Ishac, 2001). Table 1 presents the default parameters of the model.

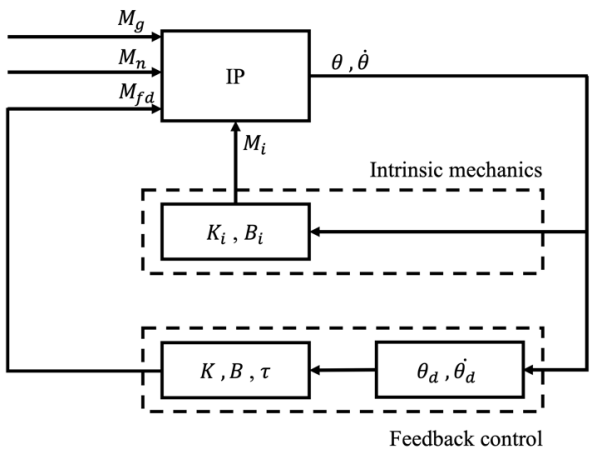

Figure 1. Inverted pendulum model with feedback. IP represents the inverted pendulum with continuously changing angular (θ) and angular velocity ($\dot{\theta}$) as the system's states. The intrinsic mechanics generates an intrinsic moment (M_i) based on the current θ and $\dot{\theta}$ and the intrinsic stiffness (K_i) and damping (B_i). In the feedback mechanism, θ_d, $\dot{\theta}_d$ represent the dead zone for angular and angular velocity respectively, acting as switches determining whether feedback control is activated. When a "switch" turns on, the feedback mechanism generates a moment (M_{fd}) based on the time-lagged IP state with feedback position gain (K) and feedback velocity gain (B) and time delay (τ). M_n and M_g represent moments generated by sensorimotor noise and gravity, respectively.

Mathematically our model takes the form of :

$$I * \ddot{\theta}_i = M_{g_i} + M_{n_i} + \left(K_i * \theta_i + B_i * \dot{\theta}_i\right) + \left(K * \theta_{i-\tau} \times H\left(|\theta_{i-\tau}| > \theta_{d_{i-\tau}}\right) + (B * \dot{\theta}_{i-\tau} \times H\left(\left|\dot{\theta}_{i-\tau}\right| > \dot{\theta}_{d_{i-\tau}}\right)\right) \quad (1)$$

Where I represents the inertia, $\ddot{\theta}$ is the angular acceleration. M_g and M_n represent the gravitational and sensorimotor noise moment, K_i and B_i are the intrinsic stiffness and damping, θ and $\dot{\theta}$ represent the angle and angular velocity, i represents the current time. H is the Heaviside function with θ_d , $\dot{\theta}_d$ the magnitude of the dead zones. The third term $\left(K_i * \theta_i + B_i * \dot{\theta}_i\right)$ represents the moment generated by intrinsic mechanics without time delay. The last term $\left(K * \theta_{i-\tau} \times H\left(|\theta_{i-\tau}| > \theta_{d_{i-\tau}}\right) + (B * \dot{\theta}_{i-\tau} \times H\left(\left|\dot{\theta}_{i-\tau}\right| > \dot{\theta}_{d_{i-\tau}}\right)\right)$ is the moment generated by time-lagged feedback control , with K and B as the feedback position and velocity gains and τ representing the delay.

Table 1. IP simulation parameters.

	Default value	Variations	Unit
$\boldsymbol{mass}$	80	-	kg
$\boldsymbol{height}$	1.8	-	m
$\boldsymbol{radius}$	0.15	-	m
$\boldsymbol{g}$	9.81	-	m/s^2
$\boldsymbol{K_i}$	1.6	70%, 100%, 350%, 600%	Nm/deg
$\boldsymbol{B_i}$	0.43	50%, 100%, 200%, 450%	Nms/deg
$\boldsymbol{K}$	16.9	60%, 100%, 120%	Nm/deg

B	5.8	60%, 100%, 110%	Nms/deg
θ_d	0.23	0, 100%	deg
$\dot{\theta}_d$	0.29	0, 100%	deg/s
M_n	10	80%, 100%, 120%	Nm
τ	150	70%, 100%, 130%	ms

To better understand which model parameters influence the estimated feedback parameters and evaluate their effects, a comprehensive variation of the model parameters was performed. Specifically, the feedback parameters were maintained within the reported range from Peterka's study. For intrinsic parameters, given the wide range of reported values across different studies, we adjusted them to be slightly higher than the lower bound and slightly lower than the upper bound to avoid extreme combinations in the model simulations. Each parameter was independently varied across the ranges specified in Table 1, resulting in a total of 5184 unique parameter combinations. For each combination, the model was simulated for 60s and this was repeated 10 times to ensure reliability. Although we narrowed the range of parameters, there were still some inappropriate combinations that generated too large sway or even instability. Simulations with sway amplitude exceeding 0.1 rad were excluded which was the maximum mean sway (5.58 deg) reported by Winter et al. (2001), resulting in 4933 valid simulations for further analysis.

Based on equation (1), we obtained the total moment exerted on the IP model, from which we calculated angular acceleration. Then we used simple Euler integration, with integration steps of 2ms to obtain the angular velocity and angle. Using the simulated data, we further calculated the kinematics of the IP center of mass (i.e., position, velocity, and acceleration) and the ground reaction force in AP direction (F_{AP}) by Newton's second law.

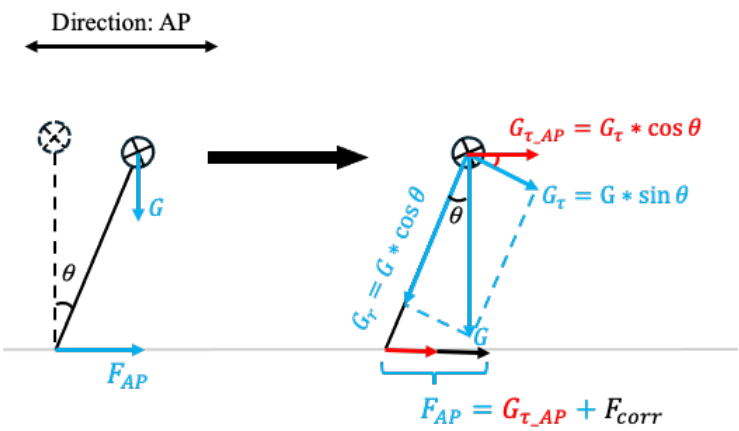

Figure 2. Calculation of corrective ground reaction force. The left plot represents the IP state, with the dashed line indicating a perfectly upright state perpendicular to the horizontal ground, while the solid line shows a representative IP state with a sway angle θ. In this representative state, the IP experiences the gravitational force (G) and generates a ground reaction force (F_{AP}) in AP direction. Due to the sway angle,

F_{AP} includes both the corrective ground reaction force (F_{corr}) and a force resulting from the gravitational component in same direction. The right plot further explains how to calculate F_{corr}. The gravity can be decomposed into two components: the centripetal force (G_r), which equals $G * \cos\theta$, and the shear force (G_τ), which equals $G * \sin\theta$. The effect of G_τ in the AP direction(G_{τ_AP}) can be calculated as $G_\tau * \cos\theta$, representing the gravitational component along the AP direction. Then the F_{corr} can be calculated as $F_{AP} - G_{\tau_AP}$.

Due to sensorimotor noise, the IP model will not maintain a vertical position but sways with ankle angle (θ). As a result, the obtained F_{AP}, is not equal to the corrective force (F_{corr}), as shown in Figure 2. Because we aimed to focus on feedback effects, we isolated the corrective force by subtracting the gravitational component in the AP direction from the total ground reaction force (Figure 2). Then, the feedback was estimated by a simple linear relationship between preceding center of mass kinematics and the corrective ground reaction force:

$$F_{corr_i} = \hat{K} * PCOM_{i-\hat{\tau}} + \hat{B} * VCOM_{i-\hat{\tau}} + \epsilon_i \tag{2}$$

Where i represents the current time, $\hat{\tau}$ is the estimated feedback delay with unit s, F_{corr} represents the corrective ground reaction force generated by feedback control, $PCOM$ and $VCOM$ are the COM position and velocity accordingly. The $\hat{K}$ and $\hat{B}$ are the estimated position and velocity gains with unit N/m and Ns/m, respectively. ϵ represents the residual error.

Using the simulated PCOM, VCOM and calculated F_{corr}, we estimated the feedback model's control parameters ($\hat{\tau}, \hat{K}, \hat{B}$) and evaluated the model's goodness of fit using the coefficient of determination (R^2). We considered F_{corr} to be sufficiently reconstructed when $R^2 \geq 0.5$ (Safavynia & Ting, 2013). The delay at which the model achieved the maximum R^2 was regarded as the feedback delay, $\hat{K}$ and $\hat{B}$ at this delay were considered as the best estimates of the actual feedback parameters. The resulting parameter estimates were averaged over the ten repetitions for further analysis. In the next step, we fitted our feedback model using human experimental data.

Experimental design & data collection

17 healthy young subjects participated in this study, of which 14 were included in the final data analysis (27± 2 yrs, 66 ± 13 kg, 1.74 ± 0.10 m). Data from two participants were excluded due to technical errors encountered during data collection, and an additional participant's data excluded following the identification of outliers in subsequent analyses. The experimental procedure was approved by the ethics committee of the Faculty of Behavioural and Movement Sciences, Vrije Universiteit Amsterdam. All participants received oral and written task instructions and signed written consent before the experiment.

We assessed three standing postures (Figure 3). 1) Normal standing: standing naturally with feet together. 2) Unipedal standing: subjects chose their preferred leg to support body weight, as previously no differences were observed between standing on the dominant or non-dominant leg (Muehlbauer, Mettler, Roth, & Granacher, 2014). 3) Step posture: this posture was determined by asking subjects to take a natural step as if walking normally at least three times until they confirmed to have reached the most comfortable step length and width. Body weight was evenly distributed between both feet. Foot positions were then marked to ensure consistency across trials.

For all postures, subjects were instructed to face forward and keep their arms naturally at their sides, trying to keep as still as possible. The normal standing trial lasted 5 minutes and was repeated twice, while the other trials lasted 1 minute and were each repeated five times. Sufficient rest time was given between tasks to avoid fatigue. To avoid bias, tasks were performed in random order. Trials in which stability was lost, i.e., touching the ground with the other leg in unipedal standing, abnormal body sway in normal standing or step posture, were repeated.

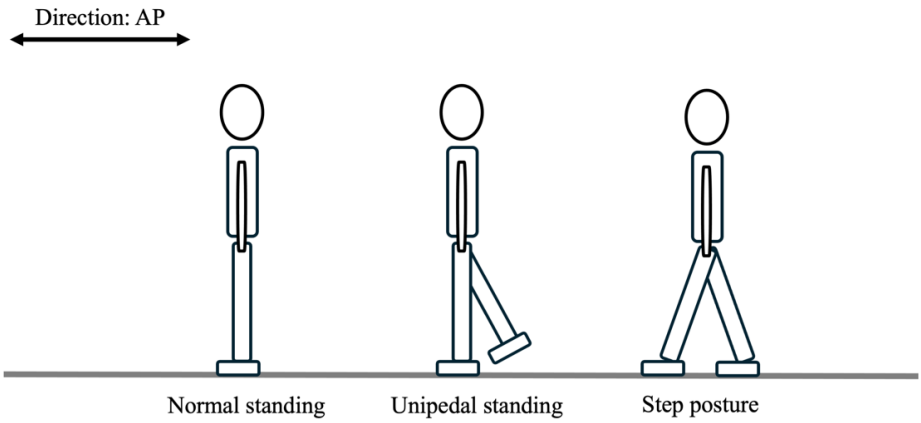

Figure 3. Sagittal plane depiction of the standing postures assessed.

Whole-body 3D kinematic data were collected at 50 sample/s using two Optotrak cameras (Northern Digital Inc., Waterloo, Ontario, Canada), with cluster markers attached to the feet, shanks, thighs, pelvis, thorax, upper arms, forearms and head. Ground reaction forces were measured with force plates embedded in the treadmill that subjects were standing on (Motek-Force-link, Amsterdam, Netherlands), and were recorded at a sampling rate of 1000 samples/s.

Raw kinematic and force data were processed using Matlab (2024a, The MathWorks, Natick, US). The PCOM was calculated using a 3D linked segment model developed by Kingma, deLooze, Toussaint, Klijnsma, and Bruijnen (1996).

VCOM was calculated as the time derivative of PCOM. Both kinematic and force data were low-pass filtered using a second-order Butterworth filter with a cut-off frequency of 10 Hz, and the force data were down-sampled to 50 Hz. To estimate the corrective ground reaction forces (F_{corr}) from the experimental data, the gravity component was subtracted as described Figure 2.

For normal standing, the first 5s and last 25s of each trial were trimmed, and the remaining 270s data were separated into three 90s parts to minimize the effect of drift during prolonged standing. For the other postures, we excluded the first 5s and last 10s of each trial. We then fitted the feedback model (equation (2)) to the experimental data. For each trial of each task, model fit (R^2), feedback delay ($\hat{\tau}$) and gains ($\widehat{K}$ and $\widehat{B}$) were estimated, and the means of these over trials were used for further analysis.

Because estimated feedback gains are strongly influenced by the body's inertial properties (Edwards, 2007; Peterka, 2002), normalization was performed for position gain ($\widehat{K}$) and velocity gain ($\widehat{B}$). The position gain ($\widehat{K}$) was normalized by dividing by mg/l where l is the height of COM above the ankle (note that this is actually a combination of two operations; first, converting the linear position gain into an angular one by means of multiplying by l^2, and then dividing this angular gain by the critical stiffness mgl). The normalized position gain $\widehat{K_n}$ is unitless and describes how many times greater the rotational stiffness is compared to the critical stiffness. Similarly, the velocity gain ($\widehat{B}$) was normalized by dividing by I/l^2, where I is the moment of inertia of the body with respect to the ankle calculated by Steiner's Law. This normalization converted the linear velocity gain into an angular velocity gain $\widehat{B_n}l^2$, then divided by inertia. The normalized velocity gain ($\widehat{B_n}$) has a unit of s^{-1}, representing the angular damping per unit of inertia over time.

Data analysis

All data from subjects that agreed to share deidentified data and code will be shared via a public repository upon acceptance of the manuscript.

Model simulations

We performed a linear regression analysis to investigate the relationship between actual and estimated feedback parameters in our model simulations after standardization (converting to z-scores by subtracting the mean and dividing by the standard deviation), the coefficient of determination (R_L^2) was reported to describe model fit. Independent variables were the intrinsic parameters (i.e.,K_i, B_i), feedback parameters (i.e.,K, B, τ), sensorimotor noise (M_n) and dead zone (θ_d, $\dot{\theta}_d$), the dependent variables were the estimated feedback delay ($\hat{\tau}$), position gains ($\widehat{K}$) and velocity gains ($\widehat{B}$).

Human experimental data

We used a one-way RM-ANOVA to compare model fit (R^2) and normalized feedback parameters (i.e., $\widehat{\tau_n}, \widehat{K_n}, \widehat{B_n}$) between standing postures. Significant main effects were followed up by Bonferroni post-hoc tests. Furthermore, to better understand any differences between postures, we determined the standard deviations of PCOM and VCOM in each of the postures. All statistical analyses were performed in MATLAB (2024a, The MathWorks, Natick, US). Results were presented as mean values with standard deviations (mean ± SD).

Results

model simulation

Simulation results demonstrated the model's effectiveness in estimating feedback control during quiet standing. The model fit (R^2) was between 0.50 and 0.99 across different parameter conditions (Figure 4) and the estimated parameters showed strong correlations with the actual parameters (Figure 5).

Linear regression results indicated that the estimated parameters were predominantly influenced by the IP's actual feedback parameters. The estimated feedback delay ($\hat{\tau}$) strongly correlated with the actual delay (τ), with a standardized regression coefficient of 0.87 ($p<0.001$). The estimated position gain ($\widehat{K}$) showed high correspondence with the actual position gain (K), with a standardized coefficient of 0.74 ($p<0.001$). The estimated velocity gain ($\hat{B}$) demonstrated a strong relationship with the actual velocity gain (B), having a standardized coefficient of 0.94 ($p<0.001$). These correlations close to identity (standardized regression coefficients close to 1) between the estimated and actual feedback parameters showed the validity of our model, suggesting that our feedback model can be used to evaluate human feedback control. Nevertheless, other parameters also affected the estimated parameters, see Table 2. Most notably, the estimated delay was influenced by actual velocity gain and intrinsic damping with standardized coefficients higher than 0.2. Estimated position gain was also influenced by intrinsic stiffness with a standardized coefficient of 0.60. Moreover, the estimated velocity gain was also influenced by both intrinsic stiffness and damping with standardized coefficients higher than 0.2. This does emphasize that our model estimates the lumped contribution of all stabilizing mechanisms and that parameters are to some extent biased if interpreted as reflecting feedback properties only.

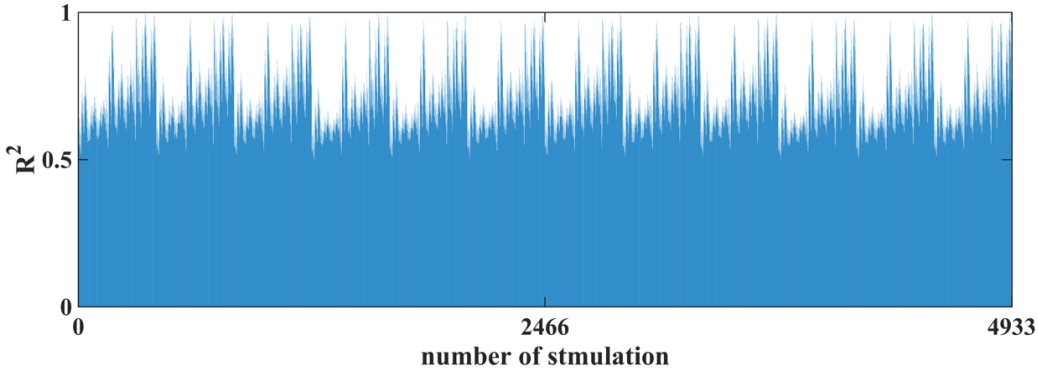

Figure 4. Model simulation results. Model fit (R^2) across all simulations, with x-axis representing the number of simulations, each simulation uses a different combination of parameters.

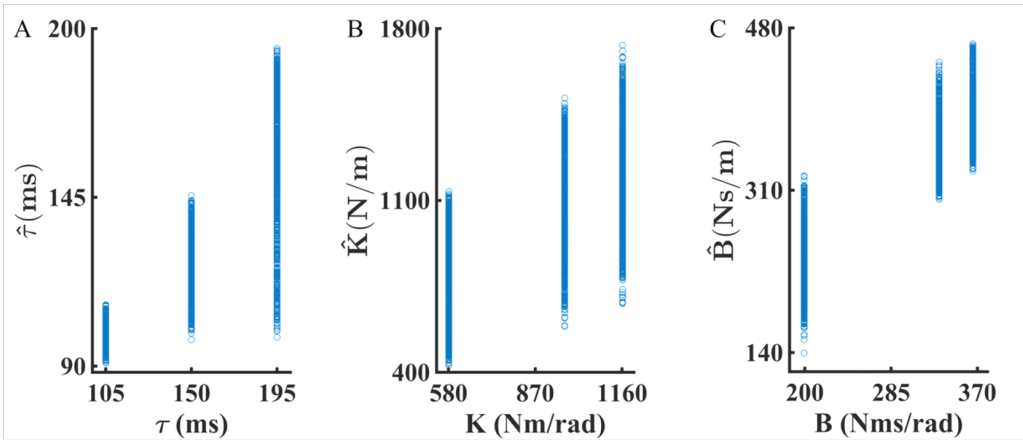

Figure 5. Estimated feedback control parameters from an inverted pendulum model with parameters varied according to Table 1. Figure 5. A-C illustrate the relationships between estimated feedback delay ($\hat{\tau}$) and actual delay (τ), the estimated position gain ($\hat{K}$) and actual position gain (K), and estimated velocity gain ($\hat{B}$) and actual velocity gain (B), respectively.

Table 2. Standardized regression coefficients. The dependent variables are shown in the first column, with $\hat{\tau}$, $\hat{K}$ and $\hat{B}$ being the estimated feedback delay, position and velocity gains. The independent variables are listed in the first row, with τ, K, B being the actual feedback delay, position and velocity gains, K_i, B_i the intrinsic stiffness and damping, M_n the sensorimotor noise, θ_d and $\dot{\theta}_d$ the position and velocity dead zone. R_L^2 is the coefficient of determination of the linear regression model. The numbers within the table represent standardized regression coefficients, with asterisks indicating levels of significance, where * indicates $p < 0.05$ and ** indicates $p<0.001$.

	τ	K	B	K_i	B_i	M_n	θ_d	$\dot{\theta}_d$	R_L^2
$\hat{\tau}$	0.87**	<-0.01	0.22**	-0.12**	-0.24**	-0.01**	0.03**	<-0.01	0.90
$\hat{K}$	0.11**	0.74**	-0.06**	0.60**	-0.14**	0.08**	-0.20**	<-0.01	0.95
$\hat{B}$	-0.19**	-0.06**	0.94**	0.22**	0.23**	<-0.01	0.02**	-0.01**	0.98

Human experimental data

Consistent with our simulation results, the variations of F_{corr} in human experimental data could be effectively reconstructed from preceding PCOM and

VCOM data for all postures performed in our study. The best model fit was observed during normal standing, with a significantly higher R^2 of 0.97±0.02, compared to the other two postures ($F_{2,26}$ = 13.5, p<0.001, Figure 6. A). In the unipedal standing, the model performance was slightly lower (R^2=0.90±0.04), while the least good fit occurred in step posture (R^2=0.90 ±0.06).

The estimated feedback delays showed significant differences between all three postures ($F_{2,26}$ = 23.6, p<0.001, Figure 6. B). The delay was largest during normal standing (246±21ms), followed by unipedal standing (204±24ms), while the smallest delay was observed in step posture (193±29ms).

The position gains exceeded critical stiffness for all postures and participants, (i.e. $\widehat{K_n}$ < -1, Figure 6.C), but were close to critical stiffness and were not different between conditions ($F_{2,26}$=1.7, p=0.2). This was surprising, as position gains were similar even between bipedal and unipedal standing while having one or two legs as actuators to control the COM.

Similarly, the velocity gains remained consistent across postures ($F_{2,26}$=1.9, p=0.17; see Figure 8), with all $\widehat{B_n}$ smaller than -2.

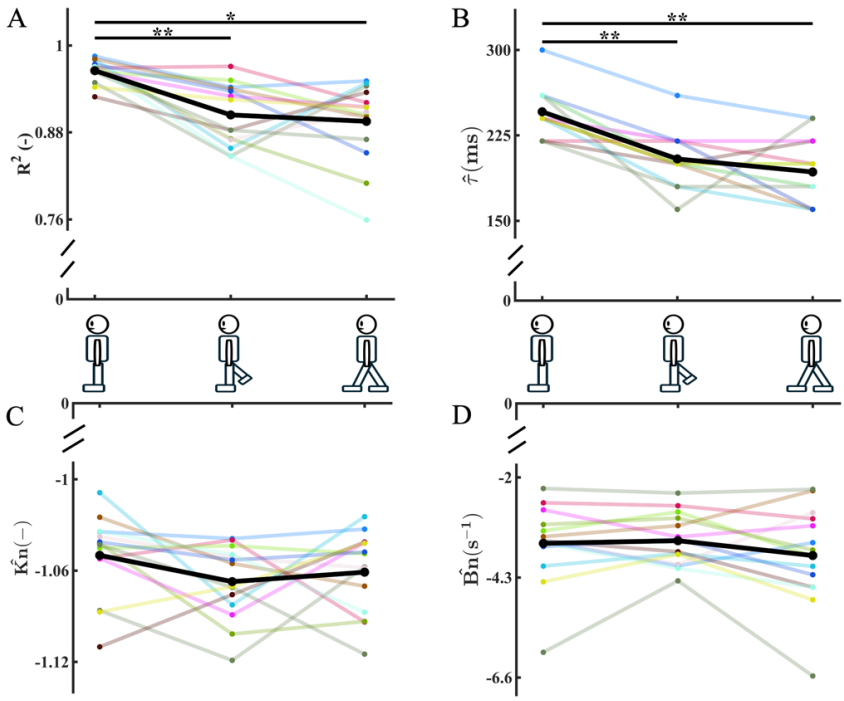

Figure 6. Results from human experimental data. Fit of the model (panel A) and corresponding feedback parameters: delay (panel B), normalized position gain (panel C), and normalized velocity gain (panel D) for normal standing, unipedal standing and step posture. Means are represented by black dots, which are connected by bold black lines, while significant differences are marked with asterisks (**: p < 0.001, *: p < 0.05). Different colors correspond to data from different subjects.

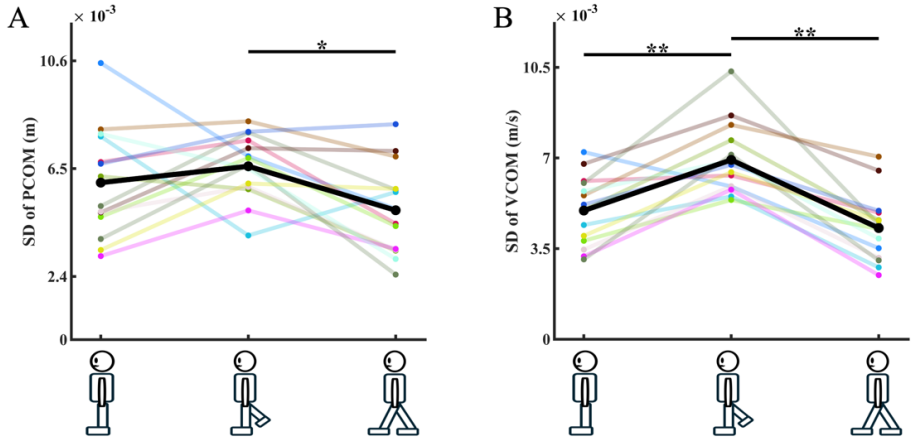

Figure 7.Standard deviation (SD) of PCOM and VCOM. SD of center of mass position (panel A) and center of mass velocity (panel B) in normal standing, unipedal standing and step posture. Means are represented by black dots and connected by bold black lines, while significant differences are marked with asterisks (**: $p < 0.001$, *: $p < 0.05$). Different colors correspond to data from different subjects.

Differences in the magnitude and velocity of postural sway between postures may have contributed to differences in goodness of fit of the model. The SD of PCOM was significantly larger in unipedal standing (0.007±0.001) compared to the step posture (0.005±0.002), with the SD in normal standing (0.006±0.002) falling in between and not significantly different from the other two postures (Figure 7. A). The SD of the VCOM was highest in unipedal standing (0.007±0.001), significantly larger than in normal standing (0.005±0.001) and step posture (0.004±0.001). While the step posture exhibited the smallest velocity variability, slightly below that of normal standing, these differences were not significant (Figure 7B).

Discussion

We proposed a simple linear regression model to represent the feedback control of human upright standing, assuming that stabilization can be achieved by generating corrective ground reaction force based on preceding center of mass kinematics. Both simulation and experimental results validated our model, such that feedback parameters could be estimated.

While previous research has used various models to explore feedback control involved in standing stability (Afschrift et al., 2021; De Groote et al., 2017; Morasso, 2022; Peterka, 2002; Vette, Masani, Nakazawa, & Popovic, 2010), to the best of our knowledge, this is the first study that quantified the relationship between horizontal ground reaction forces and COM position and velocity in unperturbed standing.

Model validity tested in simulation

Our model effectively reconstructed corrective ground reaction forces using center of mass position and velocity information (R^2: 0.50~0.99). Linear regression analysis showed estimated control parameters closely matched actual feedback parameters with standardized regression coefficients ranging from 0.74 to 0.98. This acceptable model fit and strong alignment between estimated and actual parameters validates the model's ability to estimate feedback control in human standing, despite variations of intrinsic properties, sensorimotor noise and intermittent control. Nevertheless, the effects of intrinsic parameters on estimated feedback gains, which follows from the lumped control model used, illustrates that bias in the estimates must be considered when interpreting these estimates in terms of feedback control exclusively. We do note that intrinsic parameters were varied over a substantially wider range than the feedback parameters, therefore we believe that our simulation results represent a worst-case scenario.

Modeling feedback with human data

The consistently good model fit (R^2>0.76) across all conditions of all subjects validates our model's capacity to capture human postural mechanics and suggests a common control principle across different standing postures. Normal standing yielded the best model fit compared to unipedal and step postures, possibly indicating stronger reliance on feedback control in this neutral bipedal upright posture. This aligns with previous research demonstrating maximal feedback-mediated contribution near natural bipedal standing (Mirbagheri, Barbeau, & Kearney, 2000; Nichols & Houk, 1976). The lower model fit in unipedal standing, accompanied by larger center of mass variability, suggests that additional control mechanisms beyond our feedback model may contribute more to stabilization in balance-demanding postures.

Feedback delay

The estimated feedback delay in human data ranged from 193±29ms in the step posture to 246±21ms in normal standing, falling within the peak reflex contribution timing window of 150~300ms after the onset of stretch (Sinkjaer, Toft, Andreassen, & Hornemann, 1988), supporting the physiological plausibility of our feedback model. Feedback delays were significantly shorter in unipedal standing and step posture compared to normal standing. Our simulations suggested that increased intrinsic stiffness and damping can lead to such shorter delay estimates.

This interpretation aligns with known biomechanical characteristics of these postures. In unipedal standing, the significantly higher co-contraction levels (Wu et al., 2024) and larger ankle torque contribute to increased intrinsic stiffness (Amiri & Kearney, 2019; Baratta et al., 1988; Fok et al., 2021; Sakanaka et al., 2018; Sakanaka, Lakie, & Reynolds, 2021). While in the step posture, ankle angles in both front and rear legs are non-neutral. These non-neutral ankle

angles coincide with higher intrinsic stiffness compared to normal standing, due to the non-linear relationship between ankle angle and elastic parameters (Weiss, Kearney, & Hunter, 1986). In addition, the geometric configuration of the legs in the step posture likely has larger mechanical stability in AP direction. The non-aligned angle axes will yield 'structural stiffness', enhancing the overall stiffness. In addition to bias in the estimates of the delay due to differences in the intrinsic stiffness, especially in unipedal standing, higher muscle activity can be expected to cause a shorter electro-mechanical delay (Vos, Harlaar, & van Ingen Schenau, 1991), contributing to a shorter overall delay.

Feedback gains

The estimated position ($\widehat{K_n}$) and velocity gains ($\widehat{B_n}$) remained consistent across different standing postures, revealing robust feedback control mechanisms despite varying biomechanical challenges related to the geometry (normal standing vs step posture) and number of actuators (unipedal vs bipedal standing). The normalized position gains were consistently maintained slightly below -1, exceeding the critical stability threshold as previously observed (Peterka, 2002). This near-critical stability control suggests that the CNS minimizes unnecessary muscle activation while maintaining stability.

A key finding is that position gains remained consistent despite the transition from bipedal to unipedal standing. Given that the muscular capacity available for generating corrective forces is halved in unipedal standing, this consistency in normalized gains indicates an effective doubling of feedback gain per leg, highlighting the control system's adaptability to stability demands.

Limitations

Some limitations of this study should be mentioned. Firstly, our analysis focused on feedback control in the anteroposterior direction, while particularly unipedal standing imposes greater stability demands in the mediolateral direction. The control mechanisms and parameters might be different for mediolateral control. Secondly, while we observed consistent gains across postures suggesting a doubling of gain per leg in unipedal standing, we didn't measure gain per leg, which prevents us from conclusively confirming this relationship and limits our understanding of how the control parameters changed. Thirdly, due to the lack of physiological measurements (e.g., EMG, EEG) we cannot directly link the observed control parameters with neuromuscular activity. Fourth, the calculation of corrective forces depends on the assumption that body can be modeled as an inverted pendulum and the normalization of estimated feedback gains assumed that postural sway is limited to small angles. Finally, the lumped model used can lead to bias in the estimated feedback gains, which after all reflect the lumped effect of all stabilizing mechanisms.

Conclusion

Our simple linear regression model provides a valuable framework for characterizing feedback control in human standing, demonstrated by high model fits (R^2 >0.50 in simulations, >0.76 in human data) and strong correlations (standardized coefficients >0.74) between estimated and actual feedback parameters.

Importantly, the consistency in feedback gains across postures and the fact that position gains were only slightly above critical stiffness indicate efficient control, ensuring stability, while minimizing unnecessary muscle activation.

Acknowledgements

The authors would like to give thanks to all the subjects for their participation in the experiment and her colleagues for the help during the experiments. Yang Geng was funded by China Scholarship Council (No.202309370005).

References

Afschrift, M., De Groote, F., & Jonkers, I. (2021). Similar sensorimotor transformations control balance during standing and walking. *PLoS Comput Biol, 17*(6), e1008369. doi:10.1371/journal.pcbi.1008369

Amiri, P., & Kearney, R. E. (2019). Ankle intrinsic stiffness changes with postural sway. *J Biomech, 85*, 50-58. doi:10.1016/j.jbiomech.2019.01.009

Amiri, P., Mohebbi, A., & Kearney, R. (2019). Experimental Methods to Study Human Postural Control. *J Vis Exp*(151). doi:10.3791/60078

Asai, Y., Tasaka, Y., Nomura, K., Nomura, T., Casadio, M., & Morasso, P. (2009). A model of postural control in quiet standing: robust compensation of delay-induced instability using intermittent activation of feedback control. *PLoS One, 4*(7), e6169. doi:10.1371/journal.pone.0006169

Baratta, R., Solomonow, M., Zhou, B. H., Letson, D., Chuinard, R., & D'Ambrosia, R. (1988). Muscular coactivation. The role of the antagonist musculature in maintaining knee stability. *Am J Sports Med, 16*(2), 113-122. doi:10.1177/036354658801600205

Casadio, M., Morasso, P. G., & Sanguineti, V. (2005). Direct measurement of ankle stiffness during quiet standing: implications for control modelling and clinical application. *Gait Posture, 21*(4), 410-424. doi:10.1016/j.gaitpost.2004.05.005

De Groote, F., Allen, J. L., & Ting, L. H. (2017). Contribution of muscle short-range stiffness to initial changes in joint kinetics and kinematics during perturbations to standing balance: A simulation study. *J Biomech, 55*, 71-77. doi:10.1016/j.jbiomech.2017.02.008

de Vlugt, E., van Eesbeek, S., Baines, P., Hilte, J., Meskers, C. G., & de Groot, J. H. (2011). Short range stiffness elastic limit depends on joint velocity. *J Biomech, 44*(11), 2106-2112. doi:10.1016/j.jbiomech.2011.05.022

Edwards, W. T. (2007). Effect of joint stiffness on standing stability. *Gait Posture, 25*(3), 432-439.

doi:10.1016/j.gaitpost.2006.05.009

Fok, K. L., Lee, J. W., Unger, J., Chan, K., Musselman, K. E., & Masani, K. (2021). Co-contraction of ankle muscle activity during quiet standing in individuals with incomplete spinal cord injury is associated with postural instability. *Sci Rep, 11*(1), 19599. doi:10.1038/s41598-021-99151-w

Kelton, I. W., & Wright, R. D. (1949). The Mechanism of Easy Standing by Man. *Australian Journal of Experimental Biology and Medical Science, 27*(5), 505-515. doi:DOI 10.1038/icb.1949.49

Kingma, I., deLooze, M. P., Toussaint, H. M., Klijnsma, H. G., & Bruijnen, T. B. M. (1996). Validation of a full body 3-D dynamic linked segment model. *Human Movement Science, 15*(6), 833-860. doi:Doi 10.1016/S0167-9457(96)00034-6

Latash, M. L., & Zatsiorsky, V. M. (1993). Joint Stiffness - Myth or Reality. *Human Movement Science, 12*(6), 653-692. doi:Doi 10.1016/0167-9457(93)90010-M

Loram, I. D., Gollee, H., van de Kamp, C., & Gawthrop, P. J. (2022). Is Intermittent Control the Source of the Non-Linear Oscillatory Component (0.2-2Hz) in Human Balance Control? *IEEE Trans Biomed Eng, 69*(12), 3623-3634. doi:10.1109/TBME.2022.3174927

Loram, I. D., & Lakie, M. (2002). Direct measurement of human ankle stiffness during quiet standing: the intrinsic mechanical stiffness is insufficient for stability. *J Physiol, 545*(3), 1041-1053. doi:10.1113/jphysiol.2002.025049

Milton, J., Townsend, J. L., King, M. A., & Ohira, T. (2009). Balancing with positive feedback: the case for discontinuous control. *Philos Trans A Math Phys Eng Sci, 367*(1891), 1181-1193. doi:10.1098/rsta.2008.0257

Mirbagheri, M. M., Barbeau, H., & Kearney, R. E. (2000). Intrinsic and reflex contributions to human ankle stiffness: variation with activation level and position. *Exp Brain Res, 135*(4), 423-436. doi:10.1007/s002210000534

Morasso, P. (2022). Integrating ankle and hip strategies for the stabilization of upright standing: An intermittent control model. *Front Comput Neurosci, 16*, 956932. doi:10.3389/fncom.2022.956932

Muehlbauer, T., Mettler, C., Roth, R., & Granacher, U. (2014). One-leg standing performance and muscle activity: are there limb differences? *J Appl Biomech, 30*(3), 407-414. doi:10.1123/jab.2013-0230

Nichols, T. R., & Houk, J. C. (1976). Improvement in linearity and regulation of stiffness that results from actions of stretch reflex. *Journal of Neurophysiology, 39*(1), 119-142. doi:10.1152/jn.1976.39.1.119

Pai, Y. C., & Patton, J. (1997). Center of mass velocity-position predictions for balance control. *J Biomech, 30*(4), 347-354. doi:10.1016/s0021-9290(96)00165-0

Peterka, R. J. (2002). Sensorimotor integration in human postural control. *Journal of Neurophysiology, 88*(3), 1097-1118. doi:10.1152/jn.2002.88.3.1097

Rack, P. M., & Westbury, D. R. (1974). The short range stiffness of active mammalian muscle and its effect on mechanical properties. *J Physiol, 240*(2), 331-350. doi:10.1113/jphysiol.1974.sp010613

Ribeiro, G. A., Knop, L. N., & Rastgaar, M. (2020). Multi-Directional Ankle Impedance During Standing Postures. *IEEE Trans Neural Syst Rehabil Eng, 28*(10), 2224-2235. doi:10.1109/TNSRE.2020.3018650

Safavynia, S. A., & Ting, L. H. (2013). Long-latency muscle activity reflects continuous, delayed sensorimotor feedback of task-level and not joint-level error. *Journal of Neurophysiology, 110*(6), 1278-1290. doi:10.1152/jn.00609.2012

Sakanaka, T. E., Gill, J., Lakie, M. D., & Reynolds, R. F. (2018). Intrinsic ankle stiffness during standing increases with ankle torque and passive stretch of the Achilles tendon. *PLoS One, 13*(3), e0193850. doi:10.1371/journal.pone.0193850

Sakanaka, T. E., Lakie, M., & Reynolds, R. F. (2021). Individual differences in intrinsic ankle stiffness and their relationship to body sway and ankle torque. *PLoS One, 16*(1), e0244993. doi:10.1371/journal.pone.0244993

Sinkjaer, T., Toft, E., Andreassen, S., & Hornemann, B. C. (1988). Muscle stiffness in human ankle dorsiflexors: intrinsic and reflex components. *Journal of Neurophysiology, 60*(3), 1110-1121. doi:10.1152/jn.1988.60.3.1110

van Dieen, J. H., Bruijn, S. M., & Afschrift, M. (2024). Assessment of stabilizing feedback control of walking: A tutorial. *J Electromyogr Kinesiol, 78*, 102915. doi:10.1016/j.jelekin.2024.102915

Vette, A. H., Masani, K., Nakazawa, K., & Popovic, M. R. (2010). Neural-mechanical feedback control scheme generates physiological ankle torque fluctuation during quiet stance. *IEEE Trans Neural Syst Rehabil Eng, 18*(1), 86-95. doi:10.1109/TNSRE.2009.2037891

Vos, E. J., Harlaar, J., & van Ingen Schenau, G. J. (1991). Electromechanical delay during knee extensor contractions. *Med Sci Sports Exerc, 23*(10), 1187-1193. Retrieved from https://www.ncbi.nlm.nih.gov/pubmed/1758296

Weiss, P. L., Kearney, R. E., & Hunter, I. W. (1986). Position dependence of ankle joint dynamics--I. Passive mechanics. *J Biomech, 19*(9), 727-735. doi:10.1016/0021-9290(86)90196-x

Welch, T. D., & Ting, L. H. (2008). A feedback model reproduces muscle activity during human postural responses to support-surface translations. *Journal of Neurophysiology, 99*(2), 1032-1038. doi:10.1152/jn.01110.2007

Winter, D. A., Patla, A. E., Rietdyk, S., & Ishac, M. G. (2001). Ankle muscle stiffness in the control of balance during quiet standing. *Journal of Neurophysiology, 85*(6), 2630-2633. doi:10.1152/jn.2001.85.6.2630

Wu, F., Zhang, J., Yang, K., Li, Y., Li, Z., Li, T., & Li, J. (2024). Surface electromyography analysis of ankle flexor and extensor activity under different standing stability levels. *J Orthop Surg (Hong Kong), 32*(2), 10225536241258336. doi:10.1177/10225536241258336